Retrofitting of Industrial Olefin Polymerization Plants: Producing Broad MWDs Through Multiobjective Periodic Operation

MÁRCIO NELE, JOSÉ CARLOS PINTO

Programa de Engenharia Química/COPPE, Universidade Federal do Rio de Janeiro, Cidade Universitária, CP:68502, Rio de Janeiro, 21945-970 RJ, Brazil

Received 25 May 1999; accepted 29 October 1999

ABSTRACT: The drop-in of metallocene catalysts (MCs) in existing industrial polymerization plants is the current goal of most polymer producers. However, the narrow molecular weight distribution (MWD) of the polymers produced by MCs prevent them of moving into commodities market dominated by conventional Ziegler–Natta catalysts, where ease of processing is an essential property. Broader MWDs may be obtained through mixing of different MCs or blending of different resins, but resin-compatibility problems and complex undesirable catalyst interactions pose technological problems that have yet to be solved. For these reasons, modern olefin polymerization plants have to work with both catalysts to respond to market demands, resulting in costly operations of grade/catalyst change. In this article, we describe how periodic control of short residence-time reactors operating with an MC ($Me_2Si(2\text{-}Me\text{-}Benz[e]Ind)_2ZrCl_2$/MAO) can lead to polymers with broad MWD and, consequently, to high processability. © 2000 John Wiley & Sons, Inc. J Appl Polym Sci 77: 437–452, 2000

Key words: metallocene; retrofitting; broad molecular weight distribution; periodic control; multiobjective optimization

INTRODUCTION

Modeling and simulation of olefin polymerization reactors is of great practical and academic importance. Mathematical models allow the determination of optimum reactor operation conditions for certain product specifications and the range of products that may be obtained with a determined process configuration. Besides, mathematical models are of fundamental importance during the scale up of new processes, originally developed in laboratory facilities.

A great part of the academic work developed in the field of polymer reaction engineering of catalytic olefin polymerizations has been concerned with the origin of the broad molecular weight distribution (MWD) of polyolefins synthesized with conventional heterogeneous Ziegler–Natta catalysts, rather than with practical aspects of the polymerization reaction engineering of these systems. The origin of the broad MWD was attributed to increase of the mass-transfer resistance during the particle growth and to the presence of different active sites in the Ziegler–Natta catalyst. Nowadays, the latter hypothesis is the most widely accepted.[1]

Several models were developed in the open literature to describe the dynamics of growing particles. The simplest picture was originally provided by Nagel et al.,[2] who assumed that reaction

Correspondence to: J. C. Pinto (pinto@peq.coppe.ufrj.br).
Contract grant sponsors: Conselho Nacional de Pesquisa e Desenvolvimento Tecnológico (CNPq); Polibrasil Resinas SA.

Journal of Applied Polymer Science, Vol. 77, 437–452 (2000)
© 2000 John Wiley & Sons, Inc.

takes place on the external surface of the catalyst particle. The continuous polymer buildup around the catalyst would then lead to increasing mass-transfer resistance on the surface and a continuous shift of the polymerization conditions on the catalyst surface. Schmeal and Street[3] took into consideration the porous nature of the catalyst and assumed that the active sites move slowly toward the outer part of the catalyst particle as it grows, so that different active sites might be exposed to different reaction conditions, due to mass-transfer limitations in the polymer phase. This model, usually called the polymeric center model, was later modified by Schmeal and Street,[3,4] leading to the polymeric flux model, where the movement of the initially homogeneously distributed active sites is assumed to follow the convective flow of the growing polymer particle. A further refinement of the particle-growth models is the multigrain model,[5,6] where the catalyst grain is treated as a macroparticle comprising many small spherical polymer microparticles, where diffusion between and within the microparticles is considered.

Perhaps the most important results obtained with these models regard the understanding of the complex dynamic behavior presented by heterogeneous Ziegler–Natta polymerization reactors and the assessment of the importance of the catalyst particle diameter on the stability of gas-phase olefin polymerization reactors.[7–11] Besides, it was shown that the mass-transfer resistance exerts a small influence upon the final polymer properties, when compared to the influence exerted upon the final polymer by the existence of multiple active catalyst sites with different reactivities.[12] Additionally, the effect of the residence time distribution on the reaction rate and molecular properties of final polymer resins was shown to be very significant.

The academic and industrial attention in the Ziegler–Natta polymerization field has recently turned to metallocene–aluminoxane systems [metallocene catalysts (MCs)], a new class of Ziegler–Natta catalysts. Contrary to conventional Ziegler–Natta catalysts, MCs do not lead to polyolefins with broad MWDs, but to polymers with very narrow MWDs (PD $\approx$ 2.0). The narrowing of the MWD may lead to considerable improvements of properties like mechanical resistance and transparency, but has deleterious effects on the formability of the polymers. (For comprehensive reviews on the chemistry of MCs, one may refer to Brintzinger et al.,[13] Kaminsky and Arnt,[14] and Bochhman[15]).

The polymerization reaction engineering of MCs has not been deeply investigated yet. Vela Estrada and Hamielec[16] investigated homogeneous ethene polymerization with Cp_2ZrCl_2/MAO and concluded that a double-site model should be used to describe the polymerization behavior of this system.

The use of the MC in olefin polymerization plants may eventually lead to catalyst change policies in order to allow the production of polymers with improved mechanical properties (using an MC) and polymers that are easily formable (using a conventional Ziegler–Natta catalyst) to respond to different market demands. This is particularly true for relatively small companies (producing less than 500,000 metric tons), which are obliged to produce a large number of resin grades to survive. This need may cause the production of a large amount of off-specification products, as well as increasing the complexity of the plant operation. A laborious and widely lauded solution to this problem is to use a mixture of metallocene compounds to broaden the MWD and improve the polymer formability (which would increase considerably the catalyst costs). However, the mixture of different MCs may lead to nonreproducible catalyst behavior due to the high variability of the rate of polymerization of each metallocene site.[17] A simpler solution is the use of multiple polymerization reactors operating at different polymerization conditions (usually hydrogen concentration) or the use of oscillatory operation conditions. In both cases, blending of final polymer resins may be avoided, as polymer chains are blended at the molecular scale. The use of periodic operation procedures has the advantage of requiring a single reactor, which significantly simplifies process design and leads to reduced operational costs.

The periodic operation of continuous chemical reactors can improve the performance of the reacting system and allow a better design and control of the MWD in a single reactor,[18,19] which is generally very difficult to achieve at stationary operation conditions. Despite its advantages, the literature regarding the periodic control of Ziegler–Natta polymerization reactors is limited (a comprehensive review of the periodic control of polymerization reactors can be found in Meira[18]). Claybaugh et al.[20] investigated experimentally the influence of the periodical feeding of a transfer agent (hydrogen) on the propene polymerization by a $TiCl_3$ catalyst. They pointed out that the

instantaneous polymer number-average molecular weight (M_m) is a simple function of the hydrogen concentration ([H]):

$$M_m = \frac{k}{[\mathrm{H}]} \quad \text{or} \quad M_m = k\sqrt{[\mathrm{H}]} \tag{1}$$

The appropriate hydrogen-flow profile can be calculated in order to allow the production of a polymer with the desired MWD. This very simple procedure does not take into account the natural filtering effects observed in CSTR reactors.[18]

Lee and Bailey[21] investigated the combined effect of mixing conditions and periodic operation on the Ziegler–Natta ethylene polymerization, using polymerization reactor data taken from Claybaugh et al.[20] whenever possible. In investigating "bang-bang" forced oscillations in the hydrogen concentration (chain-transfer agent), they concluded that periodical variation of the chain-transfer agent concentration and imperfect mixing can significantly enlarge the MWD, when compared to the MWD attained at steady-state conditions. Besides, it was shown that continuous reactors filter oscillations/cycling signals very fast, remaining approximately time-invariant. With the other extreme situation, when oscillations are slow, the reactor remains close to the steady-state condition at each instant.

In this work, the oscillatory operation of olefin polymerization reactors operating with an MC was investigated with the objective of producing a polymer with a broad MWD. Through the simulation of the reactor operation and multiobjective optimization of the polymer properties, it was possible to obtain manipulated variable profiles (temperature, chain-transfer agent, and monomer concentration) that lead to periodical operation and the production of polypropylene (PP) with a broad MWD. It was observed that polyolefins with broad MWDs may be produced by an oscillatory operation with, preferably, short residence-time reactors and that the feasibility of this strategy depends, essentially, on the sensitivity of the polymer properties to the manipulated variables.

PARAMETER ESTIMATION

A simple kinetic scheme based on published data[16,22] was developed. The mechanism described by eqs. (2)–(6) comprises the usual steps of a polymerization reaction by Ziegler–Natta catalysts, which are activation, propagation, chain transfer, and deactivation. The activation step takes place when the methylaluminoxane (MAO) and the metallocene (Zr) are contacted. The formed active site (C^*) is then able to polymerize propene (M). The chain transfer can take place through two different steps: chain transfer to monomer and β-hydrogen elimination. The second step is predominant at lower monomer concentrations, while the first one is predominant at higher monomer concentrations. Despite of some evidence of bimolecular deactivation on metallocene-initiated polymerization,[23] for the sake of simplicity, a monomolecular process was chosen to represent the active-site deactivation:

$$\mathrm{Zr} + \mathrm{MAO} \xrightarrow{k_a} C^* \tag{2}$$

$$C^* + M \xrightarrow{k_i} P_1 \tag{3}$$

$$P_i + M \xrightarrow{k_p} P_{i+1} \tag{4}$$

$$P_i + M \xrightarrow{k_t} Q_i + P_1 \tag{5}$$

$$P_i \xrightarrow{k_d} Q_i \tag{6}$$

The experimental data presented for the propylene polymerization with Me_2Si(2-Me-Benz[e]-Ind)$_2ZrCl_2$/MAO (ref. 22) was used for parameter estimation. As the metallocene was precontacted with MAO *ex situ,* it was assumed that the catalyst was fed into the reactor in its active form (C^*). Therefore, eq. (2) of the kinetic mechanism may be neglected. Since the active complex is highly electrophilic, the insertion of the first monomer unit takes place very fast, so that this step may be regarded as instantaneous.

Using the proposed kinetic scheme, the monomer consumption in a well-stirred semibatch reactor is given by

$$R_p = k_p M^{\alpha} e^{-k_d t} \tag{7}$$

where M stands for the monomer concentration in the liquid phase; α, for the reaction order in relation to the monomer; and k_p and k_d, for the propagation rate constant and deactivation rate con-

Table I Estimated Parameters Using $R_{p_{max}}$ Data

+	Parameter	Standard Deviation
$\ln(k_{p0})$	25.51	3.56
α	1.6	0.1
$-\frac{E_p}{R}$	−7845.03	1111.5

stant, respectively. These rate constants are written in standard Arrhenius form:

$$k_p = k_{p0}e^{-E_p/RT} \tag{8}$$

$$k_d = k_{d0}e^{-E_d/RT} \tag{9}$$

A simplified parameter estimation procedure was carried out to provide a good initial guess to the polymerization model. Initially, the kinetic parameters of propagation and the reaction order were estimated using the maximum polymerization rates, using eq. (10) in the linearized form:

$$R_{p\max} = k_{p0}e^{-E_p/RT}M^{\alpha} \tag{10}$$

The results obtained (Table I) are in close agreement with those presented by Jungling et al.[22] These initial guesses were used for a standard nonlinear maximum-likelihood parameter estimation.[24] As shown in Figure 1, experimental and simulation profiles agree fairly well. Due to the model structure, increasing monomer consumption during the first moments of the polymerization cannot be described by the model; however, the activation period is very short when compared to the other steps and is not significant for the purposes of this study.

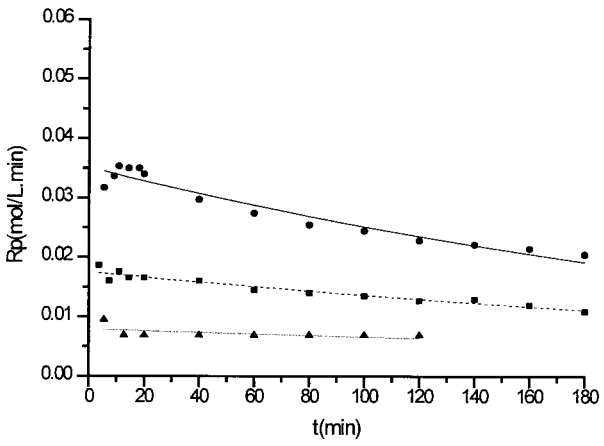

Figure 1 Comparison between experimental[22] and calculated polymerization rate data.

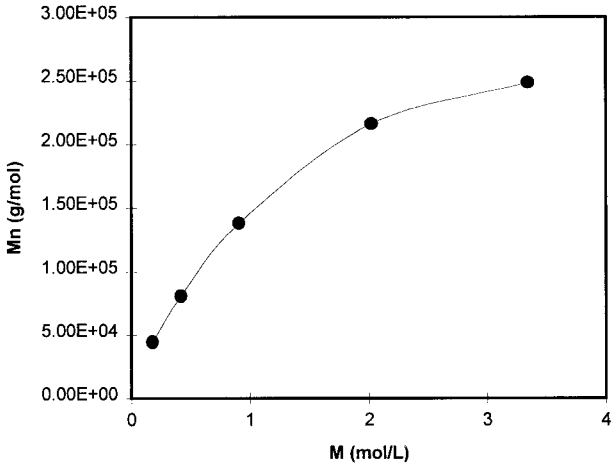

Figure 2 Effect of the concentration on the numeric-average molecular weight[22] at $T = 313$ K.

The kinetic parameters for chain transfer were estimated using eq. (11), which is valid only at stationary conditions for the chain-growth process:

$$DP = \frac{k_pM}{k_{tm}M + k_{th}} \tag{11}$$

where

$$k_{tm} = k_{tm0}e^{-E_{tm}/RT} \tag{12}$$

$$k_{th} = k_{th0}e^{-E_{th}/RT} \tag{13}$$

After linearization of eq. (11), a parameter estimation procedure was carried out using the available experimental data. The estimated rate constant for transfer to the monomer was found not to be statistically significant. However, if the dependence of the number average molecular weight on the monomer concentration is analyzed (Fig. 2), one can conclude that at higher pressures the monomer chain transfer plays a significant role. To take this dependence into consideration and keep the number of kinetic parameters low, a fractional order dependence of the molecular weight in relation to monomer concentration was devised:

Table II Kinetic Parameters

Parameter	Value	Unit
k_{p0}	2.17E + 08	$mol^{-0.6}\ L^{0.6}\ min^{-1}$
k_{d0}	0.175442	$mol\ L^{-1}\ min^{-1}$
E_p/R	7.38E + 03	K
E_d/R	1.48E + 03	K

$$DP = \frac{k_p}{k_t} M^{\gamma} = \frac{k_{p0}}{k_{t0}} e^{-\Delta E/RT} M^{\gamma} \tag{14}$$

where γ is the difference between the reaction order in relation to the propagation and transfer steps; ΔE, the difference between the activation energy of the propagation and transfer steps; and k_t, the chain-transfer rate constant that lumps the monomer chain transfer and β-hydrogen elimination. Equation (9) was then linearized and the estimated kinetic parameters were used as starting values for a nonlinear parameter estimation based on the dynamical equations that describe the system.

Based on standard kinetic assumptions, using the well-known method of moments, and taking into account the reaction order of the propagation and transfer steps, the mass balance equations may be derived from the kinetic scheme proposed as

$$\frac{d\lambda_0}{dt} = -k_d\lambda_0 \tag{15}$$

$$\frac{d\lambda_1}{dt} = -k_d\lambda_1 - k_t M^{\beta}\lambda_1 + (k_t M^{\beta} + k_t M^{\alpha})\lambda_0 \tag{16}$$

$$\frac{d\lambda_2}{dt} = -k_d\lambda_2 - k_t M^{\beta}\lambda_1 + 2k_p M^{\alpha}\lambda_1 + (k_t M^{\beta} + k_t M^{\alpha})\lambda_0 \tag{17}$$

$$\frac{d\mu_0}{dt} = (k_t M^{\beta} + k_d)\lambda_0 \tag{18}$$

$$\frac{d\mu_1}{dt} = (k_t M^{\beta} + k_d)\lambda_1 \tag{19}$$

$$\frac{d\mu_2}{dt} = (k_t M^{\beta} + k_d)\lambda_2 \tag{20}$$

where $\lambda_k = \sum_{i=1}^{\infty} i^k P_i$ is the k-th moment of the size distribution of growing polymer chains and $\mu_k = \sum_{i=1}^{\infty} i^k Q_i$ is the k-th moment of the size distribution of the dead polymer chain.

The number- and weight-average molecular weights may be obtained by numerical integration of these equations and used to estimate the transfer constant:

$$M_n = \frac{\lambda_1 + \mu_1}{\lambda_0 + \mu_0} PM \tag{21}$$

$$M_w = \frac{\lambda_2 + \mu_2}{\lambda_1 + \mu_1} PM \tag{22}$$

The transfer parameters were reestimated using the parameters obtained with eq. (14) as initial starting values. The estimated parameters do not differ significantly from the initial estimates since the steady state of the molecular weight is rapidly reached. Therefore, as long as the steady state of the molecular weight is rapidly achieved in relation to the reaction duration, eq. (14) fits fairly well the average molecular weight of the polymer produced. The parameters obtained are shown in Table II, and the excellent agreement between calculated and experimental data is shown on Figure 3. The correlation matrix (Table III) shows that there is a significant correlation between k_{p0} and E_p, and between k_{d0} and E_d. However, the correlation between the parameters of propagation and deactivation are surprisingly low, showing that these steps are physically meaningful.

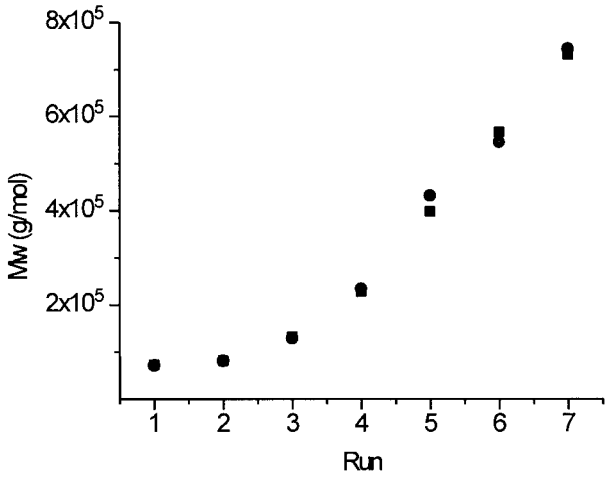

Figure 3 Comparison between (■) experimental[22] and (●) calculated weight-average molecular weight.

Table III Correlation Matrix of the Deactivation and Propagation Kinetic Parameters

	k_{p0}	k_{d0}	E_p	E_d
k_{p0}	1.00	0.71	−0.95	−0.69
k_{d0}	0.71	1.00	−0.67	−0.97
E_p	−0.95	−0.67	1.00	0.70
E_d	−0.69	−0.97	0.70	1.00

The ratio between the hydrogen chain transfer and the polymerization constant was roughly estimated using the data provided by Carvill et al.[25] It was assumed that in the presence of hydrogen, chain transfer to hydrogen is the dominant chain-transfer mechanism. The hydrogen concentration was estimated using the correlation provided by Whilhem and Battino.[26] The ratio between the monomer constant propagation and the hydrogen chain transfer at 303 K was found to be 0.23, with both monomer and hydrogen concentration expressed in mol/L.

PERIODIC CONTROL

The same kinetic scheme was used to model the continuous reactor operation. Therefore, it is assumed here that the reactor is fed with the preactivated catalyst. Assuming that the continuous reactor is an isothermal CSTR, and that the long-chain hypothesis is valid, the moment equations can be written as

$$\frac{d\lambda_0}{dt} = -k_d\lambda_0 - \frac{\lambda_0}{\theta} + \frac{P_{10}}{\theta_i} \tag{23}$$

$$\frac{d\lambda_k}{dt} = -k_d\lambda_k + k_pM^{\alpha}\left[\sum_{i=1}^{k}\binom{k}{i}\lambda_{k-1}\right] - k_tM^{\beta}\lambda_k + k_tM^{\beta}\lambda_0 - \frac{\lambda_k}{\theta} + \frac{P_{10}}{\theta_i} \tag{24}$$

$$\frac{d\mu_k}{dt} = (k_t + k_d)\lambda_k - \frac{\mu_k}{\theta} \tag{25}$$

where λ_k is the k-th moment of the size distribution of living polymer chains, and μ_k, the k-th moment of the size distribution of dead polymer chains; M, the monomer concentration (calculated with the Redlich–Kwong equation of state[27]); and P_{10}, the catalyst concentration in the feed.

Since the polymer produced by a homogeneous MC has a very low density, the volume contraction/expansion term from the global mass balance should not be disregarded if a significant amount of polymer may be produced. Assuming that the density changes due to monomer concentration are not significant when compared to variations due to the polymer produced and the reaction temperature, the total mass balance equation becomes

$$\theta = \frac{\rho\theta_i}{\rho_i - \theta_i\left[\left(\frac{\partial\rho}{\partial T}\right)\frac{dT}{dt} + \left(\frac{\partial\rho}{\partial Cpol}\right)\frac{dCpol}{dt}\right]} \tag{26}$$

where θ_i is the residence time in relation to the reactor inlet; θ, the residence time in relation to the reactor outlet; ρ, the reaction mixture density (the polymer density was taken from Brandrup and Immergut[28]); T, the reactor temperature; and $Cpol$, the polymer concentration in the reactor evaluated as *shown* in eq. (27), where PM is the monomer molecular weight. The resulting system of algebraic-differential equations (DAE) was solved using the DASSL code. Given a consistent set of initial conditions, DASSL solves the DAE over a given time interval via an implicit, adaptative-size, variable-order numerical method. The dependent variable and their derivatives are discretized via backward finite differences (BDF) formulas of one through five, and the resulting nonlinear system is solved using a modified Newton iteration[29]:

$$Cpol = (\lambda_1 + \mu_1)PM \tag{27}$$

The instantaneous polymer properties, number-average molecular weight, and polydispersion can be calculated by integration of moment equations and using the relations

$$M_n(t) = PM\,\frac{\mu_1(t)}{\mu_0(t)} \tag{28}$$

$$PD(t) = \frac{\mu_2(t)\mu_0(t)}{\mu_1^2(t)} \tag{29}$$

The problem of finding a trajectory of a control variable $u(t)$ that leads the system from its initial state to a final state such as the periodic con-

straints are satisfied may be formulated in terms of a nonlinear programming problem:

$$\text{minimize} \quad g(u) = \{\phi[u(t),\ v,\ t,\ \tau] - \phi_{\text{obj}}\}^2 \tag{30}$$

$$\text{subject to} \quad \Omega(0) = \Omega(\tau) \tag{31}$$

where Ω is the vector that defines the reactor state; g, the functional that defines the optimization goals; and ϕ, the vector containing the properties of the polymer produced during the oscillating period τ.

The properties of a polymer produced during one oscillation period (τ) can be obtained solving the DAE and averaging the moments of the MWD of the polymer effluent from the polymerization reactor. The average properties may be interpreted as if there was a surge tank at the reactor outlet where the polymer produced by the reactor is mixed and homogenized, so that the final product is a blend of all polymers produced by the reactor during the periodical cycle τ. Therefore, the final product is a blend of polymer chains produced during the periodical cycle τ. However, this blend is finely dispersed, as molecular chains with different properties are produced and mixed inside the reactor before being fed to the surge tank:

$$\bar{\lambda}_k = \frac{\displaystyle\int_t^{t+\tau} \frac{\lambda_k(t)}{\theta(t)}\, dt}{\displaystyle\int_t^{t+\tau} \frac{1}{\theta(t)}\, dt} \tag{32}$$

Equation (32) was evaluated numerically using Gaussian Quadrature.[30] The number-average molecular weight and the polydispersion can be calculated from eqs. (33) and (34):

$$\overline{M_n} = PM\, \frac{\overline{\mu_1}}{\overline{\mu_0}} \tag{33}$$

$$\overline{PD} = \frac{\overline{\mu_2 \mu_0}}{\overline{\mu_1}^2} \tag{34}$$

To carry out the optimization, the control problem was discretized and the minimization was performed over the control variable, solving the DAE over the horizon of control [0, τ] for each set of control variables suggested by the optimization algorithm. This approach, although not universally suitable, is very efficient if the solution of the DAE converges and if intermediate iterates that are either nonphysical or noncomputable are not generated.[31] To guarantee that spurious intermediate iterations were not generated, an operational window was imposed on the control variables.

The total time interval [0, τ] was divided into N equal subintervals of length Δt each, and, at each time, the discretized control variable was defined as

$$t_k = k\Delta t, \qquad k = 0,\ 1,\ \ldots,\ N \tag{35}$$

$$u(t) = u_k, \qquad k = 0,\ 1,\ \ldots,\ N \tag{36}$$

with $t_N = N\Delta t = \tau$. At each subinterval $t \in [t_k, t_{k+1}]$, $u(t)$ was defined by a C^1 piecewise shape preserving quadratic spline interpolant h_k^{32}, with nodes u_k and u_{k+1}. Shape-preserving splines keep all the continuity advantages of the spline interpolants, avoiding the need of continuity constraints in the optimization problem and precluding the oscillations present in cubic splines that lead to violation of the bound constraint, as noticed in the early stages of this work. The shape of the data points is preserved by employing monotonicity-constrained local derivative estimates and exponential tension splines. Besides, bound constraints may be applied in the spline interpolant, easing the numerical programming procedure. Furthermore, shape-constrained C^1 splines are visually similar to piecewise linear interpolants, which are easily implemented in the control practice.

The N u_k's are determined by the optimization procedure, and the operational window is defined by upper and lower bounds on the discretized control variables:

$$lb_k < u_k < ub_k, \qquad k = 0,\ 1,\ \ldots,\ N \tag{37}$$

To avoid that spline interpolants h_k's become physically meaningless (e.g., concentration less than zero), additional constraints are added to the spline generation routine:

$$lb_k < h_k(t) < ub_k, \qquad k = 0,\ 1,\ \ldots,\ N \tag{38}$$

Initially, sequential quadratic programming (SQP) method was used to find a feasible solution to the nonlinear programming problem formu-

lated above.[30] However, the method was unable to find a solution which satisfied the constraints and reasonably minimized the objective function. This behavior was ascribed to the dual characteristic of the objective function. To obtain a broad MWD, the control variable must perturb the reactor sufficiently to increase the polymer polydispersity. However, these perturbations lead to a situation where the periodic constraints may become active, so that the method gives up this new control function and keeps the reactor unperturbed.

An alternative procedure was envisaged: The periodic constraints were included in the objective function, that is, turned into a multiobjective function with the form

$$\text{minimize} \qquad f(\mathbf{u}) = \eta_1[\phi(\mathbf{u}, v, t, \tau) - \phi_{\text{obj}}]^2 + \eta_2[\Omega(0) - \Omega(\tau)]^2 \quad (39)$$

$$\text{subject to} \qquad \mathbf{lb} \le \mathbf{u} \le \mathbf{ub} \quad (40)$$

where η_1 and η_2 are weights of the objective function. To avoid scaling problems, the objective function was rewritten in a dimensionless form:

$$f(\mathbf{u}) = \eta_1 \sum_{i=1}^{k} \left(\frac{\varphi_i(\mathbf{u}, v, t, \tau)}{\varphi_{\text{obj}}} - 1 \right)^2 + \eta_2 \sum_{i=1}^{j} \left(\frac{\tilde{\omega}(0)}{\tilde{\omega}(\tau)} - 1 \right)^2 \quad (41)$$

where φ_i are the i properties of the polymer produced in each cycle; φ_{obj}, the desired value of the properties (namely, number-average molecular weight and polydispersion); and $\tilde{\omega}(0)$ and $\tilde{\omega}(\tau)$, the reactor states at $t = 0$ and $t = \tau$. The optimization procedure was applied in the equally spaced spline nodes u_k. The value of $\mathbf{u}$ at the last node (u_N) was set equal to the value at the first node (u_0), so that the optimization procedure was carried out in the $N - 1$ nodes. In the first optimization runs, the starting values of u_k were obtained by a steady-state optimization procedure on the average molecular weight, and all the u_k's were set to the result of the steady-state optimization. The weights in the objective function were initially set to unity. After finding the first minimum, the weight of the periodic constraint was set to 5–10 to fine tune the solution.

To choose the optimization method, some characteristics of the problem had to be taken into consideration. The objective function is evaluated by an adaptative integration of a DAE system and an adaptative quadrature, which makes the evaluation of the objective function expensive and sometimes noisy; the only constraint is that the control variables are bounded. The optimization was performed by the code L-BFSG,[33] which minimizes a general nonlinear function with bounds on the control variables, using gradient and function evaluations, not requiring second derivatives of the objective function that may be affected by the noise from the numerical integrations. At each iteration k, the code approximates the original problem, through a truncated Taylor Series expansion, by a quadratic subproblem (42) subject to the bound constraints (40):

$$q_k(\mathbf{u}) = f(\mathbf{u}_k) + \nabla f(\mathbf{u}_k)^T(\mathbf{u} - \mathbf{u}_k) + \tfrac{1}{2}(\mathbf{u} - \mathbf{u}_k)^T \mathbf{B}_k(\mathbf{u} - \mathbf{u}_k) \quad (42)$$

where $\nabla f(\mathbf{u}_k)$ is the gradient of the objective function at $\mathbf{u}_k$, evaluated by the forward finite difference with the Ridders extrapolation method,[30] and $\mathbf{B}_k$ is a positive definite limited memory approximation of the inverse of the Hessian matrix obtained by storing m correction pairs $\{\mathbf{s}_i, \mathbf{y}_i\}$, $i = k - 1, \ldots, k - m$, where

$$\mathbf{s}_k = \mathbf{u}_{k+1} - \mathbf{u}_k \qquad \mathbf{y}_k = \nabla f(\mathbf{u}_{k+1}) - \nabla f(\mathbf{u}_k) \quad (43)$$

These correction pairs contain information about the curvature of the function and, in conjunction with the BFGS formula, define the limited memory iteration matrix $\mathbf{B}_k$.[33]

Although the number/weight-average molecular weight and the polydispersion are widely used as a measure of the polymer quality in the polymer reaction engineering literature, it is very useful to obtain the entire MWD to access the shape of the distribution. Due to the significant computational effort involved in calculating the entire MWD, it was not used for optimization calculations. The MWD was calculated using a method based on the moments of the MWD [calculated by eqs. (23)–(26)] and on polynomial approximation. This method is described elsewhere[34] and will be only briefly outlined here.

The basic assumption of the method is that the chain-length distribution (CLD) $u_i(t)$ of a polymer at any time t can be expanded in a truncated series with the form

$$w_i(t) = \xi(i, \rho) \sum_{k=0}^{n} a_k(t, \rho) l_k(i) \tag{44}$$

where $\xi(i, \rho)$ is a strictly positive integrable reference function, which may depend on a time-dependent parameter ρ; $l_k(i)$, a set of Lagrange polynomials of the discrete variable i; and $a_k(t, \rho)$, the expansion coefficients of the CLD.

The reference function must be as close as possible to the actual distribution $w(i)$ sought in order for acceptable solutions to be obtained.[35] The choice of the reference function usually relies on some sort of *a priori* insight into the chemical process. If the MWD resembles the classical Schulz–Flory distribution, as it is usually assumed in Ziegler–Natta systems,[36] ρ has a clear physical meaning, which is associated to the propagation probability of polymer chain. Then, the final polymer MWD can be regarded as the distribution that would be obtained in a simpler situation (where the polymer chain has the same propagation probability ρ) corrected by a polynomial in order to take into account the complexity of the real system. $\xi(i, \rho)$ is obliged to satisfy the following constraints:

$$\sum_{i=1}^{\infty} \xi(i, \rho) = 1 \tag{45}$$

$$\sum_{i=1}^{\infty i} \xi(i, \rho) = \frac{\gamma_1(t)}{\gamma_0(t)} \tag{46}$$

or, more simply, if the Schulz–Flory distribution is selected as the proper reference function,

$$[1 - \rho(t)]^{-1} = \frac{\gamma_1(t)}{\gamma_0(t)} \tag{47}$$

If the moments of the distribution are calculated by the classical method of moments with sufficient accuracy, the coefficients a_k may be computed by solving the following linear system of equations:

$$\gamma_j = \sum_{i=1}^{\infty} i^j \xi(i, \rho) \sum_{k=0}^{n} a_k(t, \rho) l_k(i) s_k^j, \quad k = 0 \ldots n \text{ and } j = 0 \ldots n \tag{48}$$

To obtain an adequate approximation of the final polymer MWD, the reference distribution, weighted by the amount of polymer produced, was integrated over the oscillation period:

$$\xi[i, \rho(t)] = \int_{t}^{t+\tau} (\lambda_1(t) + \mu_1(t)) \xi^{\text{reactor}}[i, \rho(t)] dt \tag{49}$$

The MWDs presented were calculated using the first five moments calculated by integrating eqs. (23)–(26). The integral (49) was solved by simply summing up the integrand over the oscillation period. The reference distribution was calculated by introducing the first two moments of the whole polymer inside the reactor at each time t into eq. (47).

RESULTS AND DISCUSSION

The first problem that arises in the periodical reactor control is to find the cycle period τ. Initially, the oscillation period was set as a variable to be optimized; however, this strategy was not successful. In all runs, the period selected by the optimization routine was very long, leading the system from a certain steady-state condition to a second one. So, a more restrictive procedure was used, the cycle period was chosen *a priori,* and then the optimization procedure applied. By decreasing the cycle period, it is possible to determine the minimum oscillation period that still allows the proper attaining of the control objectives. A similar numerical strategy was used successfully to solve a series of optimum minimum-time control problems.[37]

Figure 4 shows the search for the minimum period. The optimized temperature profile obtained for oscillation periods of 150, 120, and 80 min, respectively, and the corresponding polydispersion of the polymer inside the reactor, that is, the variable which is most sensitive to reactor history, are shown. Desired properties were selected in order to allow the production of PP usually obtained with conventional Ziegler–Natta catalysts. It can be seen in Figure 4 that as the oscillation period decreases it becomes harder to satisfy the periodical constraint. Naturally, the minimum oscillation period also depends on the operational window imposed on the reactor. If

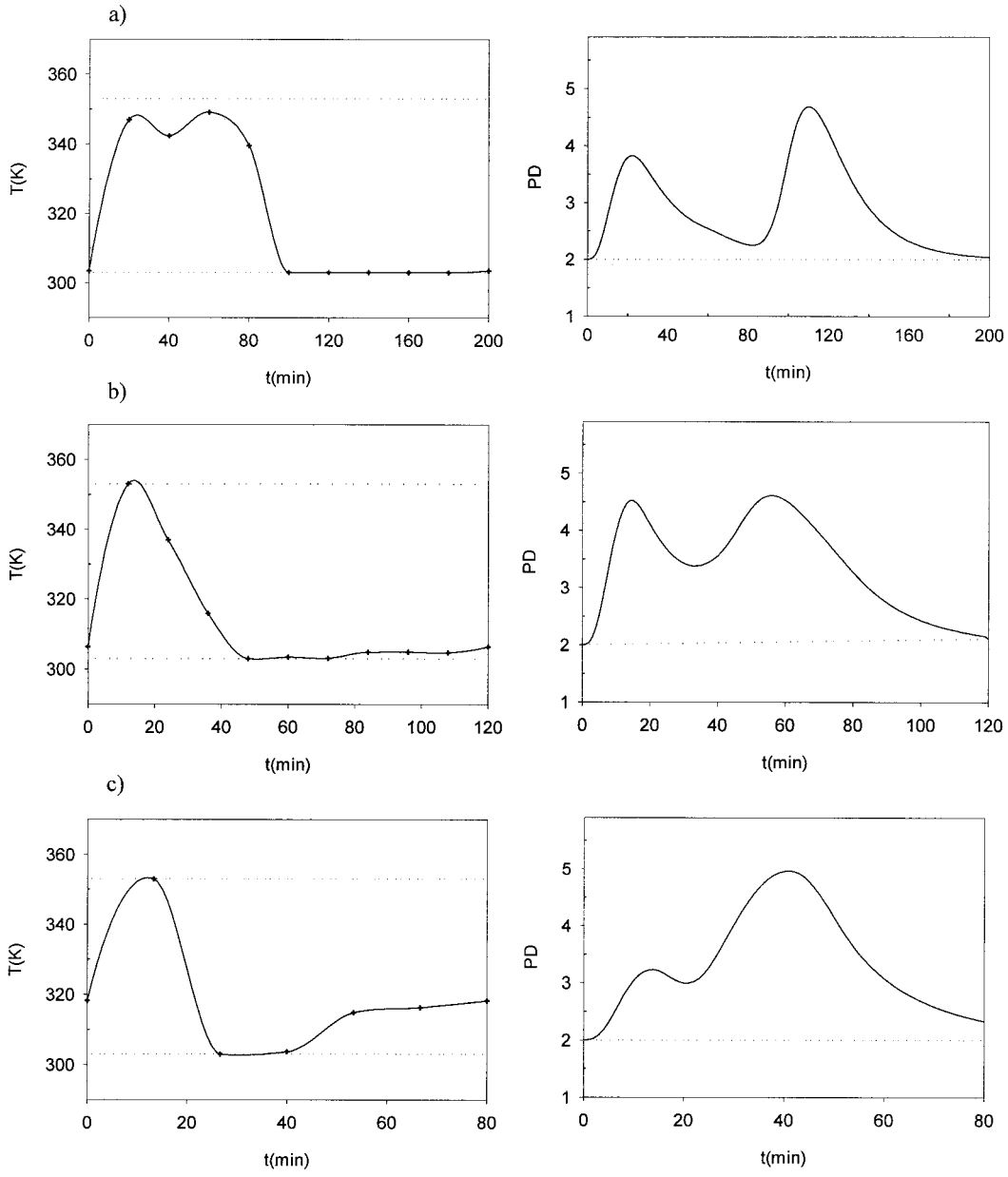

Figure 4 Search for the minimum period. Optimized temperature profile and polydispersity of the polymer inside the reactor in function of time: (a) τ = 150 min; (b) τ = 120 min; (c) τ = 80 min. Desired properties of iPP: M_n = 90,000; PD = 5.0.

this window is widened, the oscillation period may decrease significantly.

It should also be noticed that the reactor stays around the higher-temperature part of the optimized dynamic profile approximately the same time that it stays close to the lower-temperature part of the diagram. This is accomplished by manipulating the catalyst feed. If the catalyst feed is not manipulated, the reactor operates in a small time interval at higher temperature, where it can produce a large amount of polymer, and then operates in a larger amount of time at lower temperature, where the productivity, for the same catalyst concentration, is much lower. Neglecting the catalyst deactivation, the amount of catalyst (C_0) that must be fed into a continuous reactor to assure a certain productivity can be calculated by

$$R_p = P_{10} k_p M^{1.6} \tag{50}$$

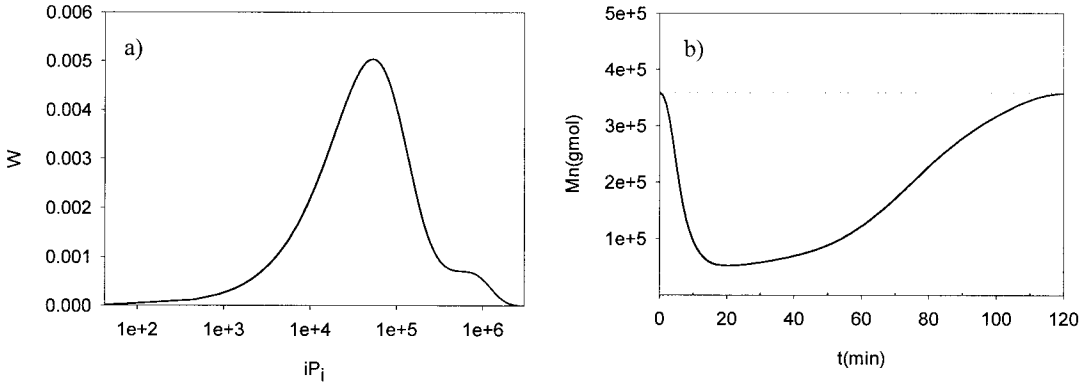

Figure 5 (a) Number-average molecular weight profile for period τ = 120 min. (b) Final MWD of the polymer producing during the oscillation period. Operating conditions: θ_i = 20 min; P = 5 bar. Desired properties of iPP: M_n = 90,000; PD = 5.0; obtained: M_n = 90,661; PD = 5.0.

where the reaction order was estimated as presented before. This means that higher catalyst concentrations are needed to keep the reaction rate constant when the reactor operates at lower temperatures, assuring a more uniform reactor productivity throughout the reactor period. It was found through extensive simulations that, as long as the reactor is not flooded by the polymer, the chosen value of R_p has little effect on the optimized profile, since the catalyst feed recipe obtained for different R_p's will differ only by a constant, if the temperature profile and the monomer concentration are kept constant.

It was found that a minimum period of 120 min is adequate to satisfy the periodic constraints and attain the optimization goals. This means that the oscillation period is of the same order of magnitude of the residence time of existing commercial processes, which guarantees that the strategy is compatible with production schedules and may be implemented in practice.

From the shape of the profiles, it may be inferred that the control variable profiles obtained with longer oscillation periods are very good starting points to the optimization procedure with smaller periods. Actually, this initialization strategy allows faster convergence and, sometimes, assures the finding of better solutions.

Figure 5 shows the evolution of the number-average molecular weight and the MWD of the final polymer. It may be seen that the final product is a molecular blend of polymer chains with significantly different sizes. More interesting, Figure 5 shows that bimodal distributions may be produced with the oscillatory operation procedure. It is known that such PP MWDs may considerably improve the end-use properties of the polymer resins.[38]

The reactor residence time is a very important variable for practical purposes. As the reactor residence time increases, the cycle period τ also increases, as it is of the same order of magnitude of the residence time. Therefore, increasing the residence time may dramatically increase the size of the surge tank necessary to homogenize the polymer produced by the reactor during the period of oscillation τ. Figure 6 shows the temperature profile obtained with a reactor with a smaller reactor residence time. The oscillation period was decreased from 120 to 80 min, even though the operational window was kept the same. Therefore, the oscillation period is better characterized in terms of the ratio between oscillation time and reactor residence time.

From a practical point of view, the manipulation of the reactor temperature is generally undesirable. First, catalysts are usually very sensitive to temperature fluctuations. As discussed before, the manipulation of the reactor temperature requires the manipulation of the catalyst feed rates, in order to keep the reactor productivity approximately constant. Second, the reactor temperature must be manipulated through manipulation of the cooling system variables, such as cooling water feed flow rates and cooling water feed temperature. Very frequently, it becomes impossible to follow the temperature policies because additional heat-transfer constraints may exist.[39] This is particularly true during the decreasing temperature time intervals, where large water feed flow rates are needed to remove the heat of reaction and additionally refrigerate the reac-

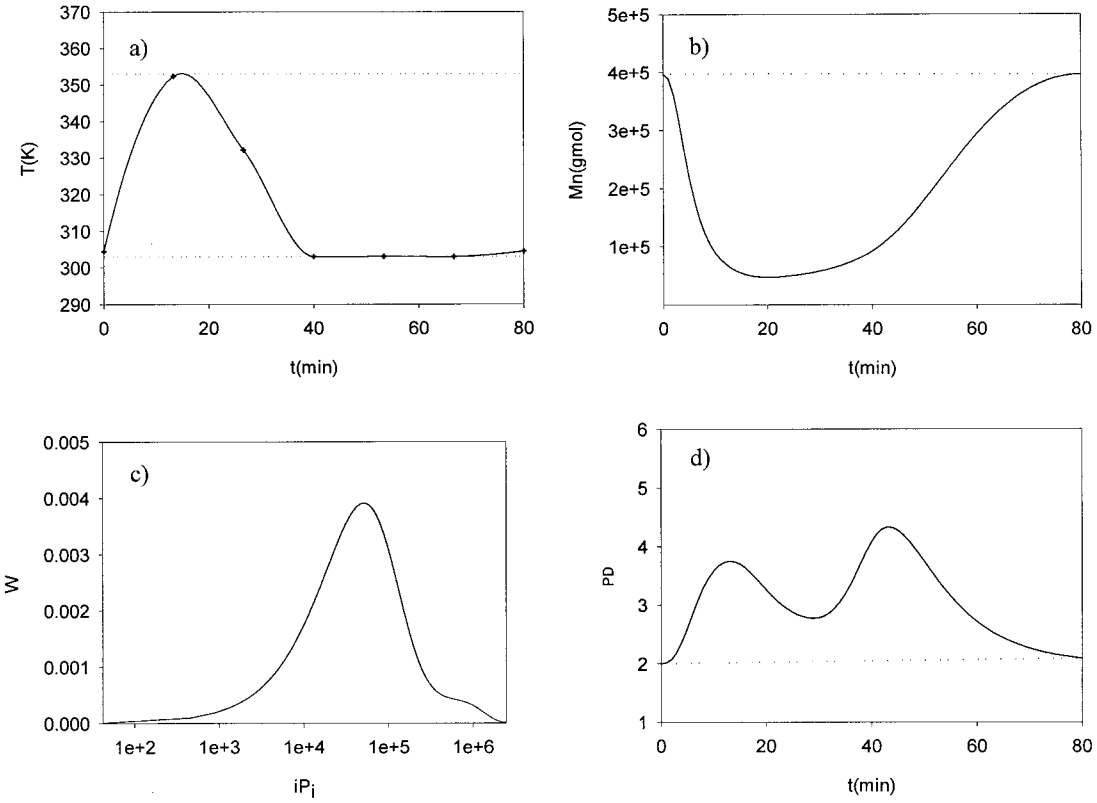

Figure 6 Effect of a smaller residence time: (a) temperature profile; (b) number-average molecular weight profile; (c) final MWD of the polymer producing during the oscillation period (τ = 80 min); (d) polymer polydispersion profile. Operating conditions: θ_i = 20 min; P = 5 bar. Desired properties of iPP: M_n = 90,000; PD = 5.0; obtained: M_n = 92,457; PD = 5.0.

tion environment. If a chain-transfer agent (hydrogen) is used to control the MWD, the implementation of the oscillatory policies may be made much simpler.

Figure 7 shows an attempt to obtain broaden MWDs using hydrogen pressure as the manipulated variable. It can be seen that the final objectives can be achieved if significant perturbations on the reactor pressure are introduced. It must be noticed that optimum profiles are roughly constituted of regions where hydrogen concentrations are kept around the operation bounds. This type of operation reduces the operation costs dramatically, as hydrogen concentrations may be easily manipulated through gas feed and gas vent lines. Besides, hydrogen may be separated from other gaseous constituents with reflux condensers and can be recirculated without much additional purification.

In spite of the previous discussion, pressure changes of 10 bars are unacceptable most of the times, which means that combination with the manipulation of other variables (reactor temperature) would be advisable in this case. Nevertheless, it must be pointed out that the magnitude of the pressure perturbations will certainly depend on the metallocene sensitivity to the presence of hydrogen, so that the magnitude of the perturbation will be smaller for metallocenes that are more sensitive to hydrogen. An increase of an order of magnitude of the transfer rates to hydrogen would approximately cause a 10-fold reduction of the pressure perturbations, which would then be acceptable for practical purposes. Therefore, it may be said that MCs that are sensitive to hydrogen concentrations are preferable for PP production.

An alternative that should not be discarded in this case would be the use of two continuously stirred tank reactors in series. The first tank would operate with hydrogen pressures around 7 bars and residence times of 80 min, while the second one would operate with hydrogen pressures around 1 bar and residence times of 40 min.

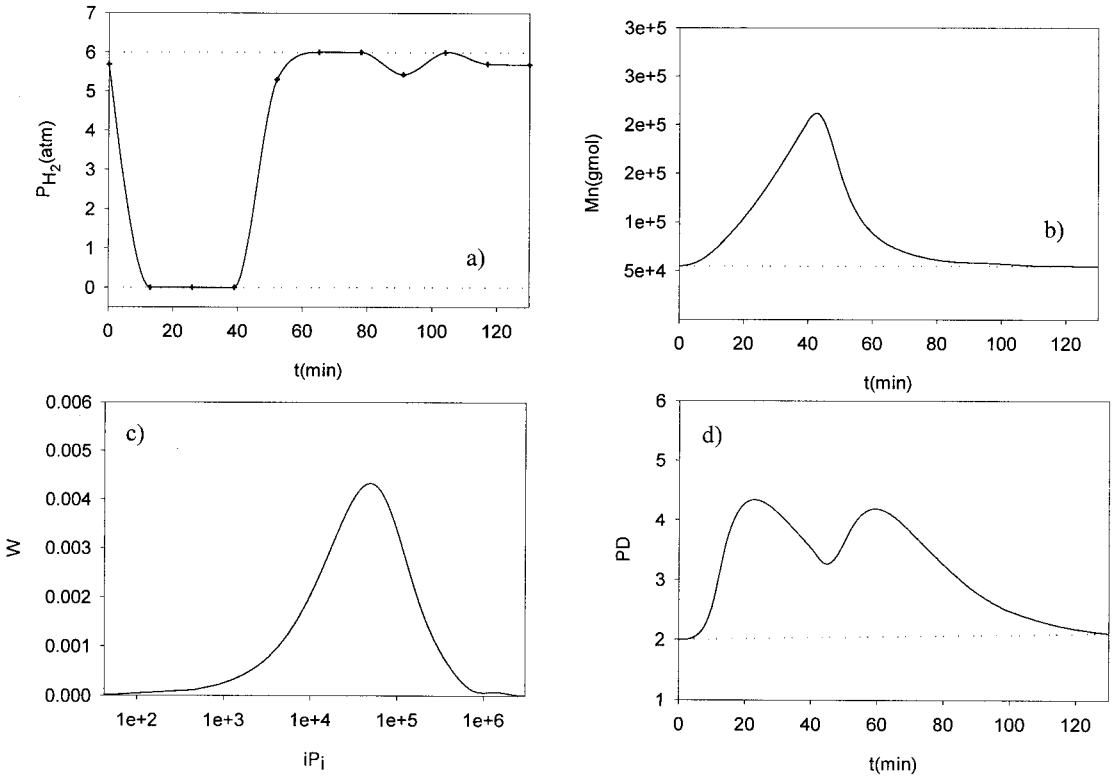

Figure 7 Manipulation of the chain-transfer agent: (a) hydrogen-pressure profile; (b) number-average molecular weight profile; (c) final molecular weight distribution of the polymer producing during the oscillation period (τ = 120 min); (d) polymer polydispersion profile. Operating conditions: θ_i = 20 min; P = 5 bar; T = 303 K. Desired properties of iPP: M_n = 90,000; PD = 5.0; obtained: M_n = 90,617; PD = 5.0.

The results obtained are very similar to the ones presented in Figure 7 because the dynamics of the growing chains is negligible. In Figure 7, the MWD of the growing chains is constant throughout the first 40 min and afterward change for a second plateau and remain approximately constant during the following 80 min. The continuous variations of average molecular weights presented in Figure 7 are due to the continuous mixture of the new polymer chains formed with the previous ones already present in the reactor. The main disadvantage of this strategy is that it does not allow the production of polymer grades with significantly higher polydispersions (unless additional reactors are added to the train), which can be carried out through the periodic operation without much difficulty.

An additional variable that can be manipulated very easily in an industrial environment is the monomer pressure (concentration). This may be achieved through manipulation of the monomer feed rate and/or manipulation of the catalyst feed rate (to keep reactor productivity stable). Figure 8 presents an attempt to produce a broad MWD through optimization of the monomer concentration. It can be seen that the reactor pressure, although easy to manipulate, does not allow the production of a polymer with very broad MWD (although a polydispersion around 3 is already adequate for fibers production[40]). This behavior is due to the nature of the chain-transfer reactions in this catalyst. At lower pressures, the dominant chain-transfer path is the β-hydrogen elimination, which does not depend on the monomer pressure, while at higher pressures, the dominant path is the chain transfer to the monomer, which is not sensitive to monomer concentration. Therefore, an important issue in the periodic control is the sensitivity of the polymer properties to the manipulated variable. This kinetic behavior is usual for MCs, so that it seems that manipulation of monomer pressures will not allow the implementation of useful control policies to widen the polymer MWD.

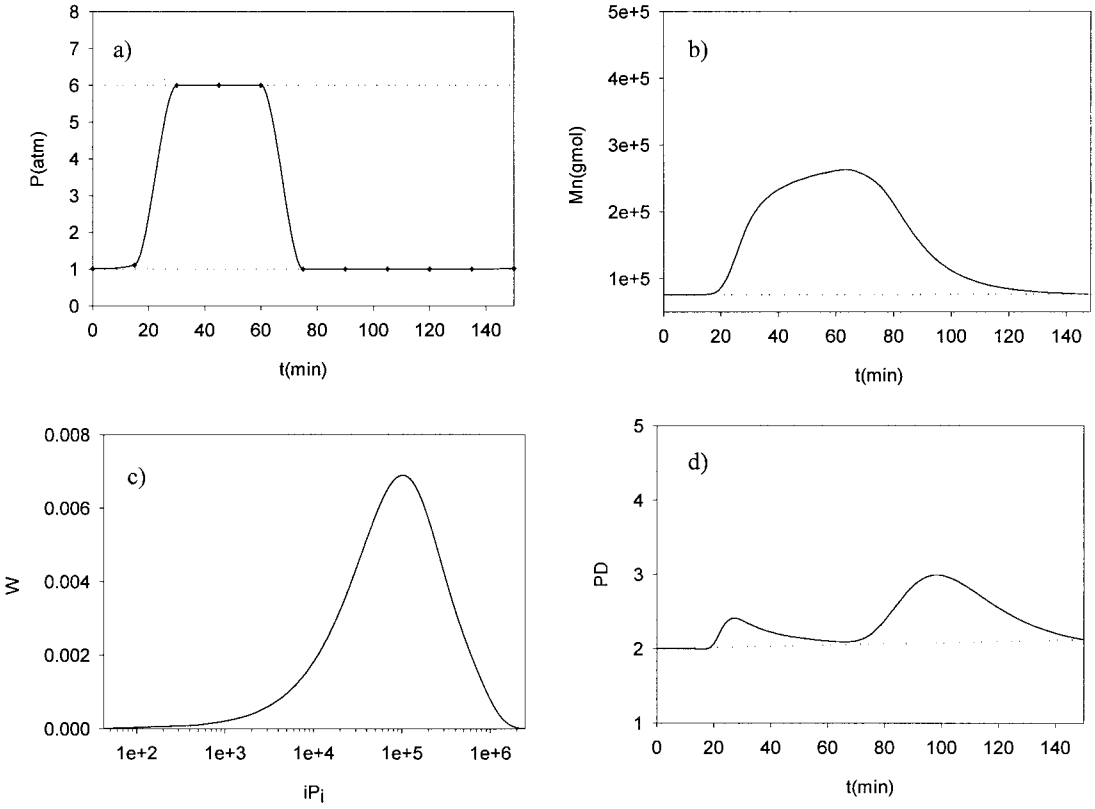

Figure 8 Manipulation of the monomer pressure: (a) hydrogen-pressure profile; (b) number-average molecular weight profile; (c) final MWD of the polymer producing during the oscillation period (τ = 120 min); (d) polymer polydispersion profile. Operating conditions: θ_i = 20 min; P = 5 bar; T = 313 K. Desired properties of iPP: M_n = 90,000; PD = 5.0; obtained: M_n = 95,350; PD = 2.7.

CONCLUSIONS

The results presented here show that the periodic operation of continuous polymerization reactors may allow the production of PP with commercial-grade polydispersions with MCs *in situ* through the proper development and implementation of temperature and hydrogen-pressure policies. Oscillation periods required were shown to be of the same order of magnitude of existing commercial processes and compatible with production schedules. Although the manipulation of hydrogen pressures is preferable, as it does not disturb polymer productivity significantly and is not limited by heat-transfer constraints, this would require the use of more sensitive MCs or the introduction of significant pressure perturbations upon the reactor operation. In this case, the use of tanks in series would probably lead to better process performance.

The authors thank the Conselho Nacional de Pesquisa e Desenvolvimento Tecnológico (CNPq) for providing scholarships and supporting our work. The authors also thank Polibrasil Resinas SA for supporting this research. The authors are indebted to Prof. Linda Petzold (DASSL), Prof. Ciyou Zhu and Prof. Jorge Nocedal (L-BFSG), and Prof. Robert J. Renka (TSPACK) for freely distributing their codes through the Netlib (http://www.netlib.org).

NOMENCLATURE

a_k	expansion coefficients
C^*	active site
$Cpol$	polymer concentration in the reactor
DP	degree of polymerization
E_d	activation energy of the propagation step
E_p	activation energy of the propagation step
E_t	activation energy of the propagation step
h_k	k-th spline interpolants
k_d	deactivation rate constant
k_{d0}	preexponential factor of the deactivation rate constant
k_p	propagation rate constant

k_{p0} preexponential factor of the propagation rate constant
k_t transfer-rate constant
k_{t0} preexponential factor of the transfer rate constant
lb_k k-th lower bound of the control variable
M monomer concentration
M_n number-average molecular weight
M_w weight-average molecular weight
P reactor total pressure without hydrogen
P_{10} catalyst concentration on the feed stream
PD polymer polydispersion
P_i living polymer chain of size i
PM monomer molecular weight
Q_i dead polymer chain of size i
R gas universal constant
R_p polymerization rate
T temperature
t_k k-th spline nodes in time
$u(t)$ control variable function
ub_k k-th upper bound of the control variable
u_k k-th spline nodes in the control variable
W polymer weight fraction
w_i polymer molecular weight distribution
Zr metallocene

Greek

α polymerization apparent reaction order
θ reactor residence time in relation to the reactor exit stream
θ_i reactor residence time in relation to the reactor feed stream
ξ_i reference molecular weight distribution
γ_i i-th moment of a molecular weight distribution
λ_i i-th moment of the living polymer chains
μ_i i-th moment of the dead polymer chains
η_i i-th weight of the objective function

Vector Quantities

lb vector containing the lower bounds of the control variable
u vector containing the spline nodes of the control variable
ub vector containing the upper bounds of the control variable

REFERENCES

1. Kissin, Y. V. Isospecific Polymerization of Olefins with Heterogeneous Ziegler–Natta Catalysts; Springer-Verlag: New York, 1985.
2. Nagel, E. J.; Nagel, V. A.; Ray, W. H. Ind Eng Chem Prod Res Dev 1980, 19, 372–379.
3. Schmeal, W. R.; Street, J. R. AIChE J 1971, 17, 1188–1197.
4. Schmeal, W. R.; Street, J. R. J Polym Sci Polym Phys Ed 1972, 10, 2173–2187.
5. Choi, K. Y.; Ray, W. H. J Appl Polym Sci 1985, 49, 1573–1588.
6. Sau, M.; Gupta, S. K. Polymer 1993, 34, 4417–4426.
7. Laurence, R. I.; Chiovetta, M. G. In Polymer Reaction Engineering: Influence of Reaction Engineering on Polymer Properties; Reichert, K. H.; Geiseler, W., Eds.; Hanser: Munich, 1983.
8. Ferrero, M. A.; Chiovetta, M. G. Polym Eng Sci 1987, 27, 1436–1447.
9. Ferrero, M. A.; Chiovetta, M. G. Polym Eng Sci 1987, 27, 1448–1460.
10. Ferrero, M. A.; Chiovetta, M. G. Polym Eng Sci 1991, 31, 886–903.
11. Ferrero, M. A.; Chiovetta, M. G. Polym Eng Sci 1987, 31, 904–911.
12. Floyd, S.; Choi, K. Y.; Tsqlor, T. W.; Ray, W. H. In Catalytic Olefin Polymerization, Studies in Surface Science and Catalysis; Keii, T.; Soga, K., Eds.; Elsevier: Amsterdam, 1986; Vol. 25.
13. Brintzinger, H. H.; Fisher, D.; Mülhaupt, R.; Rieger, B.; Waymouth, R. M. Angew Chem Int Ed Engl 1995, 34, 1143–1170.
14. Kaminsky, W.; Arnt, M. Adv Polym Sci 1997, 127, 143–187.
15. Bochmann, M. J Chem Soc Dalton Trans 1996, 3, 255–270.
16. Vela Estrada, J. M.; Hamielec, A. E. Polymer 1996, 35, 808–818.
17. D'Agnillo, L.; Soares, J. B. P.; Penlidis, A. Polym Int 1998, 47, 351–360.
18. Meira, G. R. J Macromol Sci-Rev Macromol Chem 1981, C20, 207–241.
19. Schiffino, R. S. U.S. Patent 5 475 067, 1995.
20. Claybaugh, B. E.; Griffon, J. R.; Watson, A. T. U.S. Patent 3 472 829, 1969.
21. Lee, C. K.; Bailey, J. E. AIChE 1974, 20, 74.
22. Jungling, S.; Mulhaupt, R.; Stehling, U.; Brintzinger, H. H.; Fisher, D.; Langhauser, F. J Polym Sci Part A Polym Chem 1995, 33, 1305–1317.
23. Fisher, D.; Mülhaupt, R. J Organomet Chem 1991, 417, C7–C11.
24. Noronha, F. B.; Pinto, J. C.; Monteiro, J. L.; Lobão, M. W.; Temisson, T. S. In Um Pacote Computacional para Estimação de Parâmetros e Projeto de Experimentos; Technical Report COPPE/UFRJ, Rio de Janeiro, Dec. 1993 (in Portuguese).
25. Carvill, A.; Tritto, I.; Locatelli, P.; Sacchi, M. C. Macromolecules 1997, 30, 7056–7062.
26. Wilhem, E.; Battino, B. Chem Rev 1973, 73, 1–9.

27. Reid, R. C.; Prausnitz, J. M.; Poling, B. E. The Properties of Gases and Liquids, 4 ed.; McGraw: New York, 1987.
28. Brandup, J.; Immergut, E. H. Polymer Handbook, 3rd ed.; Wiley: New York, 1989.
29. Petzold, L. R. In Scientific Computing, Stephan, R., Ed.; North-Holland: Amsterdam, 1983.
30. Press, W. H.; Teukolsky, S. A.; Vetterling, W. T.; Flannery, B. P. Numerical Recipes in Fortran: The Art of Scientific Computing, 2 ed.; Cambridge University: New York, 1992.
31. Asher, U. M.; Mattheij, R. M. M.; Russel, R. D. Numerical Solution of Boundary Value Problem for Ordinary Differential Equations; Classics in Applied Mathematics, Vol. 13; SIAM: Philadelphia, PA, 1995.
32. Renka, R. J. ACM Trans Math Soft 1993, 19, 81–94.
33. Byrd, R. H.; Peihuang, L.; Nocedal, J.; Ciyou, Z. A Limited Memory Algorithm for Bound Constrained Optimization; Technical Report NAM-08; Department of Electrical Engineering and Computer Science, Northwestern University, May 1994.
34. Nele, M.; Sayer, C.; Pinto, J. C. Macromol Theory Simul 1999, 8, 199–213.
35. Pinto, J. C.; Biscaia, E. C. Latin Am Appl Res 1996, 26, 1–20.
36. Hamielec, A. E.; Soares, J. B. P. Prog Polym Sci 1996, 21, 651.
37. Oliveira, A. T. M.; Biscaia, E. C., Jr.; Pinto, J. C. J Appl Polym Sci 1998, 69, 1137–1152.
38. Cecchin, G. Macromol Symp 1994, 78, 213.
39. Secchi, A. R.; Lima, E. L.; Pinto, J. C. Polym Eng Sci 1990, 30, 1209–1219.
40. Becker, R. F.; Burton, L. P. J.; Amos, S. E. In Polypropylene Handbook; Moore, E. P., Ed.; Hanser: New York, 1996; Chapter 4.